Intermediate-range order in aqueous solutions of salts constituted of divalent ions combined with monovalent counter-ions



2002 J. Phys.: Condens. Matter 14 7427

(http://iopscience.iop.org/0953-8984/14/32/303)

INSTITUTE OF PHYSICS PUBLISHING JOURNAL OF PHYSICS: CONDENSED MATTER

J. Phys.: Condens. Matter **14** (2002) 7427–7448 PII: S0953-8984(02)30973-1

# Intermediate-range order in aqueous solutions of salts constituted of divalent ions combined with monovalent counter-ions

**M Alves Marques, M I Cabaço, M I de Barros Marques and A M Gaspar**

Centro de Física da Matéria Condensada da Universidade de Lisboa, Av. Prof. Gama Pinto, 2, 1649-003 Lisboa, Portugal
and
Departamento de Física, Instituto Superior Técnico, Av. Rovisco Pais, 1049-001 Lisboa, Portugal

E-mail: marques@cii.fc.ul.pt, isabel@cii.fc.ul.pt, barros@cii.fc.ul.pt and agaspar@cii.fc.ul.pt

Received 20 November 2001, in final form 19 April 2002
Published 2 August 2002
Online at stacks.iop.org/JPhysCM/14/7427

**Abstract**

Concentrated aqueous solutions of salts constituted by divalent ions combined with monovalent counter-ions were investigated by x-ray diffraction and Raman spectroscopy at room temperature. The salts studied were strontium, barium, and magnesium chlorides and bromides, and lithium and caesium sulphates. For many of these solutions, intensity maxima were detected in their x-ray diffraction patterns close to 0.6–1 $Å^{-1}$. Interpretation of these maxima, *pre-peaks*, is discussed, taking into account the results of previous investigations of the authors on concentrated aqueous solutions of trivalent cations. In these solutions the *pre-peaks* appear to be narrower and much more intense. In the ionic solutions studied here, a slight contrast between values of the scattering power of two spatial domains is suggested as the origin of the observed *pre-peak*. One of these comes from an accumulation of scattering power around the ion with the higher electric charge, locally organized into a subtle close packing; the other comes from the holes of this structure. Molecular models of the structure of these electrolytes are used to demonstrate the plausibility of this interpretation.

## 1. Introduction

X-ray diffraction methods have produced a great deal of information about the distances between ions and water molecules in direct contact in aqueous solutions. These results, with varying degrees of accuracy, have been considered as giving unequivocal interpretations. The existence of medium-range ion–ion correlations, at distances of the order of 8–10 Å in concentrated aqueous solutions, has been discussed by many authors [1–21]. Some of these

  

studies involved neutron diffraction investigations [4–6, 9, 15], and have been the subject of considerable controversy [22]. A variety of aqueous ionic solutions have been studied, with the cations having an electric charge greater than, equal to, or smaller than the charge of the anion [3, 13, 17, 19–21]. An interference maximum has been observed at $Q_0$ close to 1 $Å^{-1}$ in the x-ray patterns of aqueous solutions of salts which does not exist in liquid water. The value of $Q_0$ decreases when the concentration of the solute diminishes. The dependence of $Q_0$ upon the molar concentration $c$, given by $Q_0 \propto c^{1/3}$, is in agreement with the existence of a *quasi-close packing* of the solute ions of higher valence [17]. As indicated in previous articles, we should stress that a *quasi-close packing* is a local close-packing structure (cubic face-centred) which does not go beyond the first shell of 12 neighbours around each representative point of the structure. Prins and Fonteyne [1] were the pioneers of the investigations on the presence of intermediate-range order in concentrated aqueous solutions: in x-ray photographic patterns of concentrated aqueous solutions containing heavy ions, they discovered a 'moving ring' which was interpreted as demonstrating the existence of a 'superarrangement' within these liquids.

Our analysis consists in the calculation of the scattering intensities for various models and comparing these with the experimental pattern. This method (correlation method) has proved to be appropriate for several concentrated aqueous solutions, with roughly 20 water molecules per high-valence ion. These models seem to be most successful in certain specific circumstances:

(i) the salts must be completely dissociated;
(ii) the valences of the ions that constitute the dissolved salt must be different, such that dense electronic clouds are dominantly around only one ionic species (either cation or anion).

The competition between the ions of higher valence for obtaining their maximum hydration shell seems to be a relevant condition for the existence of a *close packing*, the structure where their mutual distances are as large as possible.

The possibility of obtaining structural information by this method has been checked for concentrated aqueous solutions of metallic cations where the above requirements are satisfactorily fulfilled [3, 13, 17, 19–21]. The solubility of the salts chosen allowed us to obtain solutions where up to 20 water molecules per cation were present. Since the scattering power of the higher-valence ions is appreciably larger than that of the corresponding counter-ions and than that of the water molecules occupying a volume equal to the volume of these ions of large valence, a good visibility of interference maxima is observed. High-valence cations were preferred to anions in order to obtain a high value of the electrostatic field around the ion. Thus, indium, yttrium, and lanthanum trivalent cations were investigated in solutions of chlorides, bromides, and nitrates [13, 17, 19–21].

The results may be briefly summarized:

(i) Constructive interferences of x-rays scattered by the first-neighbour ions of high valence clearly contribute to the intensity of the maximum observed near 1 $Å^{-1}$.
(ii) These constructive interferences occur at mutual distances of the scattering entities that may be calculated considering a *close packing* of these ions present in the solution.
(iii) The free counter-ions (in this case, the anions) are located *approximately* at the middle points of the *cation–(close-neighbour) cation* distances. The x-rays scattered by counter-ions clearly interfere with those scattered by cations (contributing destructively to the maximum).
(iv) The solvation shells around the cations give scattering contributions that appreciably reinforce the constructive interferences indicated above.

The detection of positional correlations between the high-valence ions (i.e. the centres of the dense electron clouds) and between these and the counter-ions is possible because variations

of the phase differences of the x-rays scattered by the correlated ions can produce visible interference maxima and minima in the profile of the total intensity, in a region of $Q$ from $\approx$1 up to 3 Å$^{-1}$. This leads to a more straightforward interpretation of the experimental patterns while the radial distribution function is almost insensitive to variations in the correlations of ions which are not in contact (correlations up to distances of about 10 Å).

We demonstrate here the relevance of the role played by divalent ions (cations or anions) in determining a *local close packing* in liquid solutions. For this purpose concentrated aqueous solutions of magnesium, barium, and strontium chlorides and bromides, and concentrated aqueous solutions of lithium and caesium sulphates have been investigated. As stated above, the adequacy of our molecular models is clearly demonstrated if the scattering factors of the solvated ions are very large when compared with the value for liquid water; however, this does not occur with the aqueous solutions reported here. As an example, the effective scattering power [21] of the sulphate anion is nine times greater than that corresponding to an equal volume of liquid water while the effective scattering power of the hydrated lithium cation is only three times larger than that corresponding to an equal volume of liquid water. Nevertheless, even in these circumstances, interesting conclusions can be obtained from the experiments reported.

## 2. Experiment and data reduction

X-ray diffraction patterns were obtained in our laboratory (CFMCUL, Lisbon) and at the European Synchrotron Radiation Facility (ESRF, Grenoble) on beamline ID15b. Rh K$\alpha$ radiation ($\lambda = 0.615$ Å) monochromatized by reflection from a lithium fluoride crystal was used in the conventional set-up. The intensities were measured on a slightly modified Philips $\theta$–$2\theta$ horizontal goniometer with a scintillator counter. The angular range of the scattering angle covers $2^\circ \leqslant 2\theta \leqslant 103^\circ$, allowing measurements up to a momentum transfer $Q = 4\pi \sin\theta/\lambda \sim 16$ Å$^{-1}$. Several runs were accumulated with a constant number of counts at each point. At beamline ID15b, monochromatized synchrotron radiation of 88.620 keV ($\lambda = 0.140$ Å) was used, and the range 0.3 Å$^{-1} \leqslant Q \leqslant 18$ Å$^{-1}$ was covered by changing the sample–detector distance. The detection system was a MAR online image plate scanner (2300 $\times$ 2300 pixels: pixel size 0.15 mm). The one-dimensional diffraction patterns were obtained by integration of the diffraction rings of the 2D patterns.

The aqueous solutions were prepared from their hydrated salts, $MgCl_2$ and $SrCl_2$ from Merck (p.a.) and $Li_2SO_4$, $Cs_2SO_4$, $MgBr_2$, $SrBr_2$, $BaCl_2$, and $BaBr_2$ from Alfa Aesar (∼99%). The composition of the solutions was monitored by chemical analysis. Their concentrations and densities are presented in table 1. Samples were studied at room temperature by transmission either in layers of some tenths of a millimetre thick (for $\lambda = 0.615$ Å) or of some millimetres thick (for $\lambda = 0.140$ Å). These were contained in a plane-parallel cell between Kapton (25 $\mu$m thick) or nitrocellulose (30 $\mu$m) windows.

The measured intensities were corrected for background, scattering of the container and absorption. A polarization correction was also performed for the experimental results with the 1D detector. The corrected intensities were scaled to absolute units using the Krogh–Moe method [23].

Finbak's method, as reformulated by Warren [24], was applied to the experimental data and used to calculate the following total pair correlation function of the solution, $g(r)$:

$$g(r) = 1 + \left(2\pi^2 r \rho_e \sum_{\text{uc}} Z_j\right)^{-1} \int_0^{Q_{max}} Q i'(Q) \mathrm{e}^{-bQ^2} \sin(rQ)\,\mathrm{d}Q \qquad (1)$$

where $\rho_e$ is the average scattering density of the solution, $Z_j$ the atomic numbers, and $i'(Q)$ the reduced intensity defined as:

**Table 1.** Concentration, number of water molecules per divalent ion, and density of the aqueous solutions investigated.

| | Concentration (mol $dm^{-3}$) | $H_2O$ molecules per divalent ion | Density[a] (g $cm^{-3}$) |
|---|---|---|---|
| $MgCl_2$ | 4.7 | 10 | 1.32 |
| | 3.4 | 15 | 1.24 |
| $MgBr_2$ | 4.4 | 10 | 1.62 |
| $SrCl_2$ | 2.6 | 20 | 1.34 |
| | 1.3 | 42 | 1.18 |
| $SrBr_2$ | 2.9 | 17 | 1.58 |
| $BaCl_2$ | 1.5 | 36 | 1.27 |
| | 0.71 | 74 | 1.09 |
| $BaBr_2$ | 1.9 | 26 | 1.47 |
| $Li_2SO_4$ | 2.7 | 19 | 1.22 |
| $Cs_2SO_4$ | 3.5 | 12 | 1.98 |

[a] Values obtained at $20 \pm 2\,^{\circ}C$.

$$i'(Q) = \left(I_{eu}(Q) - \sum_{uc} f_j^2\right) \Big/ F^2(Q) = i(Q)/F^2(Q). \tag{2}$$

$I_{eu}(Q)$ is the total intensity and $i(Q)$ is the so-called dependent intensity.

In the sharpening factor $F(Q) = \sum_{uc} f_j / \sum_{uc} Z_j$ the sum extends over all four species in the solution. In the modification function $e^{-bQ^2}$, $b$ was set equal to 0.01 or to 0.006 $Å^2$ depending on the value used for $Q_{max}$. Different values of $Q_{max}$ were tested for both the Krogh–Moe method and the Fourier inversion. In the data analysis presented here we used $Q$-values up to 14 or to 18 $Å^{-1}$ (ESRF). This cut-off produces spurious peaks and decreases the spatial resolution, but this is not relevant for distances greater than 1 Å. A final correction has been made through the removal of spurious oscillations in the pair correlation function $g(r)$ at small distances (<1 Å). The so-called pair correlation function $g(r)$ was back-transformed in order to obtain the corrected dependent intensity. Most of the solutions have been studied with both set-ups. In general, a good agreement is obtained with a much better signal/noise ratio at high $Q$-values for the results obtained at ID15b ESRF.

The structural units in the solutions (the units of composition 'uc') are always given with reference to the divalent ion. For all the atoms, the coherent scattering factors $f_j$, corrected for anomalous dispersion, were taken from x-ray tables [25]. Incoherent scattered intensities corrected from the Breit–Dirac recoil factor were calculated from the work of Pálinkás [26] for the Br, Sr, Ba, and Cs atoms, and from Pálinkás and Radnai [27] for the Li, O, S, and Cl atom. For $H_2O$ we used the coherent scattering factors and the incoherent scattered intensity from Hajdu [28].

The Raman spectra were obtained on a Spex 1403 spectrometer with a double monochromator, a Spectra Physics 2016 $Ar^+$ laser (1 W) and a R928 Hamamatsu photon counter. The exciting line was at 488 nm and a resolution of $\sim$15 $cm^{-1}$ was used.

## 3. Results and discussion

### *3.1. Experimental results*

X-ray diffraction patterns for the most concentrated aqueous solution of each salt investigated are presented in figures 1–4. The first intensity maximum observed in the diffraction patterns

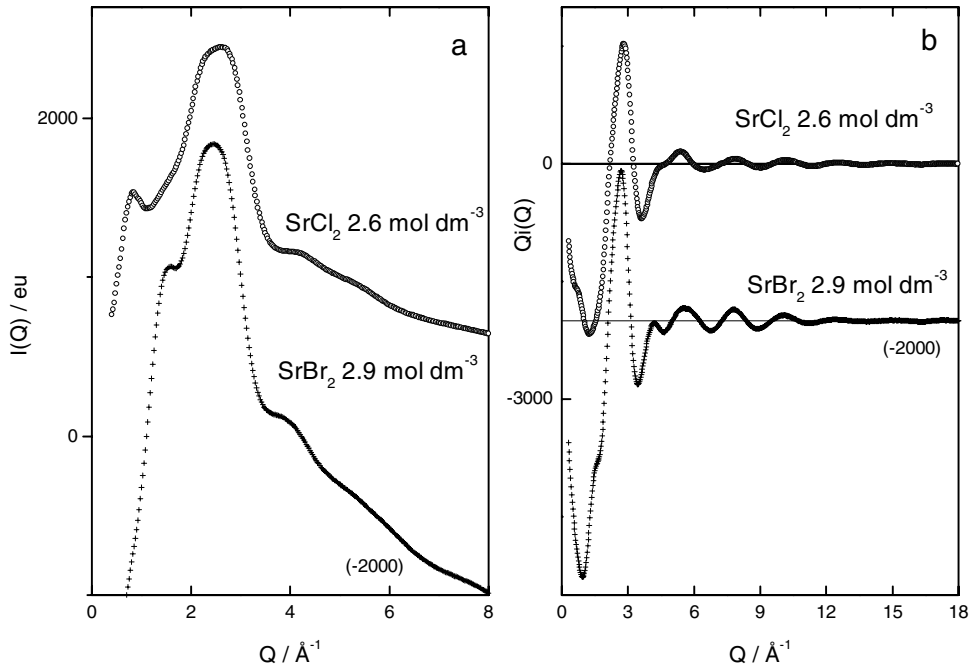


**Figure 1.** X-ray diffraction patterns of 2.6 mol dm$^{-3}$ $SrCl_2$ and 2.9 mol dm$^{-3}$ $SrBr_2$ aqueous solutions: (a) $I_{eu}(Q)$; (b) $Qi(Q)$. For clarity, the $SrBr_2$ solution curves are shifted by $-2000$ eu.

(at $Q \leqslant 1$ Å$^{-1}$) of the solutions of strontium (figure 1), barium (figure 2), and magnesium (figure 3) chlorides decreases strongly in intensity for the corresponding barium bromide solution and is not observed in the case of strontium and magnesium bromide solutions. In agreement, the shoulder observed near 1 Å$^{-1}$ in the diffraction pattern of the lithium sulphate solution cannot be distinguished in the corresponding region of the diffraction pattern for the caesium sulphate solution (figure 4).

The value of $Q_0$ for the first maximum of intensity increases with the solution concentration. This dependence for the strontium, barium, and magnesium chloride solutions can be seen in figures 5(a)–(c), while the evolution versus the power 1/3 of the molar concentration is displayed in figure 5(d). Moreover, this evolution is well described by a straight line with a slope calculated by considering that each shell of scatters (hydrated cations) is ordered as a face-centred cubic lattice.

### *3.2. Molecular models: general remarks*

Analysis of x-ray diffraction patterns of concentrated aqueous solutions of salts with ions of different valences may be interpreted by assuming the existence of a *liquid-type close packing* of the solute ions of highest valence. Competition between the ions having around them the more intense electrostatic field will lead to an (approximately) cubic structure where they are as far apart as possible in the dense arrangement required by the strong cation–anion electrostatic attraction.

The cooperative interaction of the x-rays scattered by the different ions and molecules produces a total intensity that can reasonably be computed from the Debye formula:

$$i(Q) = \sum_{j \neq k} f_j f_k \frac{\sin(Q r_{jk})}{Q r_{jk}}$$

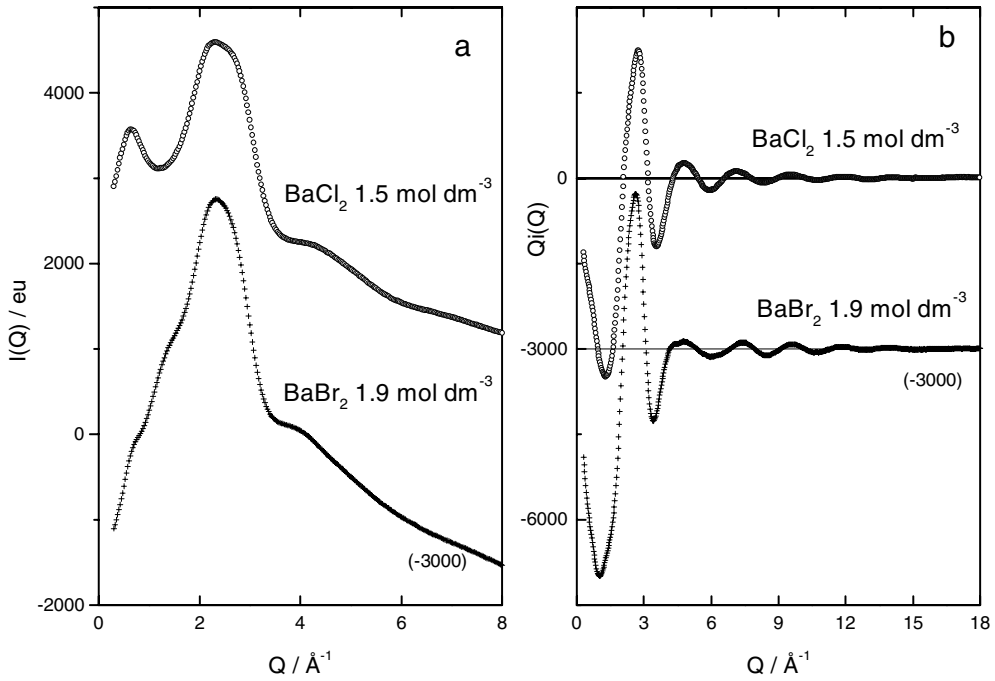


**Figure 2.** X-ray diffraction patterns of 1.5 mol dm$^{-3}$ $BaCl_2$ and 1.9 mol dm$^{-3}$ $BaBr_2$ aqueous solutions: (a) $I_{eu}(Q)$; (b) $Qi(Q)$. For clarity, the $BaBr_2$ solution curves are shifted by $-3000$ eu.

where $f_j$ are the atomic or molecular scattering factors, and $r_{jk}$ the distances between the atoms or molecules $j$ and $k$. This approximation is valid if there is spherical symmetry around each atom or molecule, which is approximately achieved within the volume of coherence of the Rayleigh scattering. The method of calculation has been described previously [1, 24, 29]. Two different internal configurations are considered in distinct regions: the first, *near the central 'particle'*, is crystalline-type (discrete distribution), while the other, which starts at a reasonable distance, threshold, from the central particle and goes up to large distances, is simulated by a random (uniform) distribution. The first region is intended to simulate the local order around each particle $j$ for which the local density is different from the bulk (density). These differences attenuate for increasing values of distances $r$, and for $r > r_{jl}^{th}$ the particle $j$ will 'see' the suggested uniform distribution which simulates, perhaps, the space average structure of the solution at these large distances. It seems certain that the thresholds $r_{jl}^{th}$ of these continua are the more important 'perspectives' in the context of the physical meaning of our model: the assemblage of their values assigned to the different types of correlation expresses the relevance of local order in an ionic solution because each threshold value represents the radius of the sphere, around each central 'particle' $j$ inside which a discrete distribution of 'particles' $k$ is idealized. The value of the intensity $i_c$ produced by the continuum starting at each threshold $r_{jl}^{th}$ should be no larger than the value $i_d$ obtained for the intensity from the discrete region in the range of $Q$-values useful for the discussion of the plausibility of the model: the role of contributions originating from a region where the arrangement of the molecules and ions is poorly known should not be overplayed. Values of the radii $r_{jl}^{th}$ of the spheres (that contain, inside, the discrete distributions around each molecule or ion $j$) are adjusted to obtain a reasonable fit to the profile of the experimental intensity. For these reasons

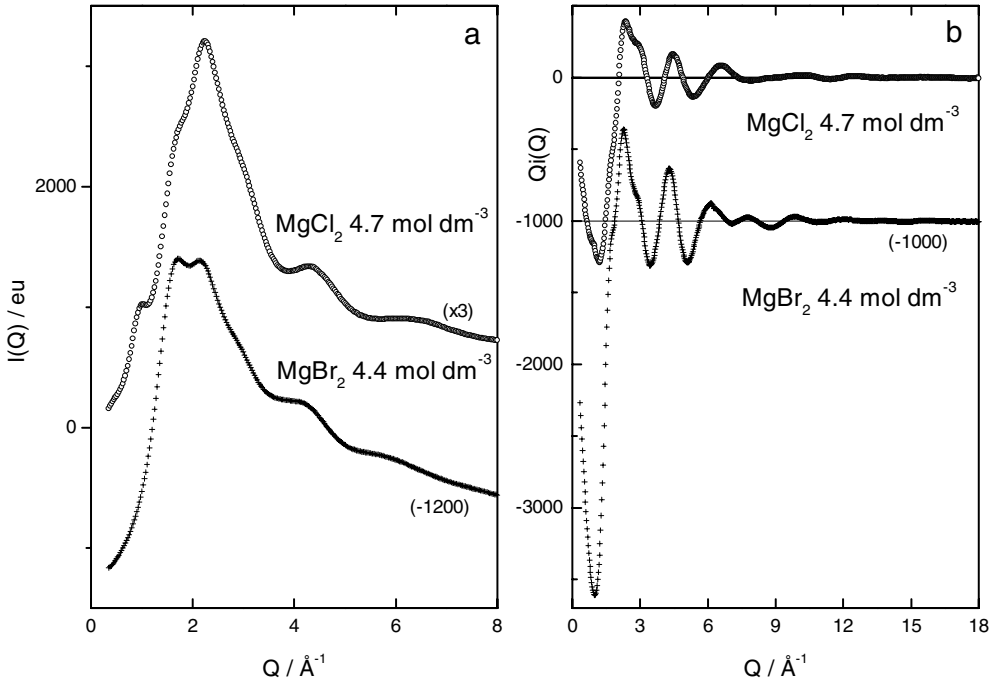


**Figure 3.** X-ray diffraction patterns of 4.7 mol dm$^{-3}$ $MgCl_2$ and 4.4 mol dm$^{-3}$ $MgBr_2$ aqueous solutions: (a) $I_{eu}(Q)$; (b) $Qi(Q)$. For clarity, the $MgBr_2$ solution curves are shifted by $-1200$ eu and in (a) the $MgCl_2$ curve appears multiplied by a factor of 3.

the calculated intensity in electron units, $I_{eu}(Q)$, corresponding to the molecular models, and idealized to interpret the profile of the observed x-ray intensity, is thought reliable only for $Q$-values above $\sim$1 Å$^{-1}$ (see the dashed curves for calculated values of $I_{eu}(Q)$ below 1 Å$^{-1}$ in figures 7–14).

The shape and the size of the first shell around the metallic cations is suggested from the Fourier inversion of the experimental intensity, and considerations from the literature described in detail in section 3.3. The ions of higher valence are located at distances given by the first neighbours in a close packing. These close-packed positions sometimes correspond to a *probability of presence* less than one, which means that the localization of the number of first neighbours is better simulated using a cooperation with a continuous distribution. Free anions and water molecules are distributed over the middle points of the two next-neighbour cations in agreement with the volume allowed by close packing, taking into account electrostatic interactions. The water molecules that cannot be located at mid-points between the cations are distributed in the available holes of this *face-centred cubic lattice* (tetrahedral and octahedral holes). In synthesis, the *scattering units* are only the hydrated cations, the anions, and *free* water molecules (those not concerned with the hydration shell).

Fluctuations of the values of the distances between the ions or molecules are assumed arbitrarily to be Gaussian, and are appropriately adjusted for each concentrated aqueous solution. The values of these fluctuations $\Delta r$ are larger for longer distances and are of the order of 15% if the correlated atoms or molecules do not belong to the same hydrate (see tables 2–5). Although the values of $\Delta r$ indicated in tables 2(a), 3(a), and 5(a) for the internal distances of cation hydrate may seem excessive, we must emphasize that the orientation of the water

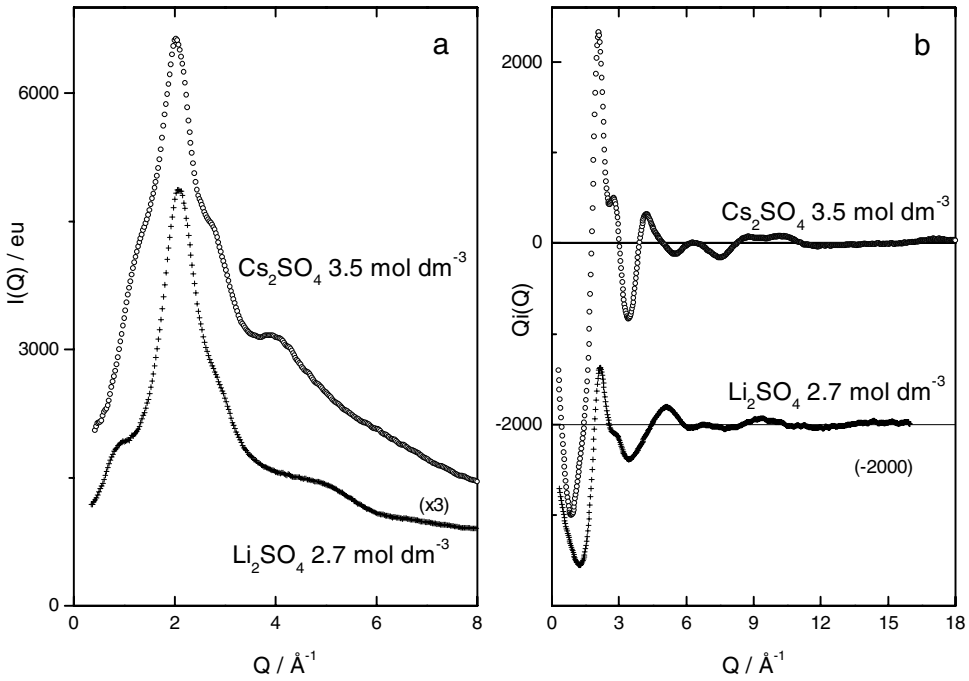


**Figure 4.** X-ray diffraction patterns of 2.7 mol $dm^{-3}$ $Li_2SO_4$ and 3.5 mol $dm^{-3}$ $Cs_2SO_4$ aqueous solutions: (a) $I_{eu}(Q)$; (b) $Qi(Q)$. For clarity, the $Cs_2SO_4$ solution curves are shifted by $-3000$ eu and in (a) the $Li_2SO_4$ curve appears multiplied by a factor of 3.

molecules in the hydrates is not very regular (taking into account the values of their relevant multipoles). Hence, a range of values of distances will be expected for the slightly different aggregates.

These molecular models give a profile of the calculated intensity that approximately fits the experimental data. The probability of presence of the high-valence first-neighbour ions in the quasi-close-packing structure suggested for the ions studied in this paper is small. For concentrated solutions of indium chloride and bromide, of lanthanum chloride and bromide, etc (solutions of salts with a trivalent cation associated with a monovalent anion), the experimental intensity may be plausibly interpreted by means of molecular models where a large number of ions and molecules belonging to all the 12 first neighbours in the close packing are considered to be integrated in a discrete distribution. In contrast, for solutions of salts with divalent ions associated with monovalent ions, exemplified here, the value of the probability of presence of the hydrated ions in the shell of the 12 first neighbours drops significantly. This is in agreement with our earlier hypothesis of the relevance of the electrostatic field in the ionic solution in the generation of the *quasi-close-packing* structure.

The physical meaning of this lack of involvement of some water molecules, or ions, in the entire first shell of neighbours of higher valence may be attributed, plausibly, to either

(i) some spatial domains of the liquid sample alternating over a period of time between two 'instantaneous' configurations (discrete and non-discrete); or
(ii) at the same instant different spatial domains of the solution exhibiting discrete and non-discrete configurations.

In an ergodic perspective these two interpretations are, of course, equivalent.

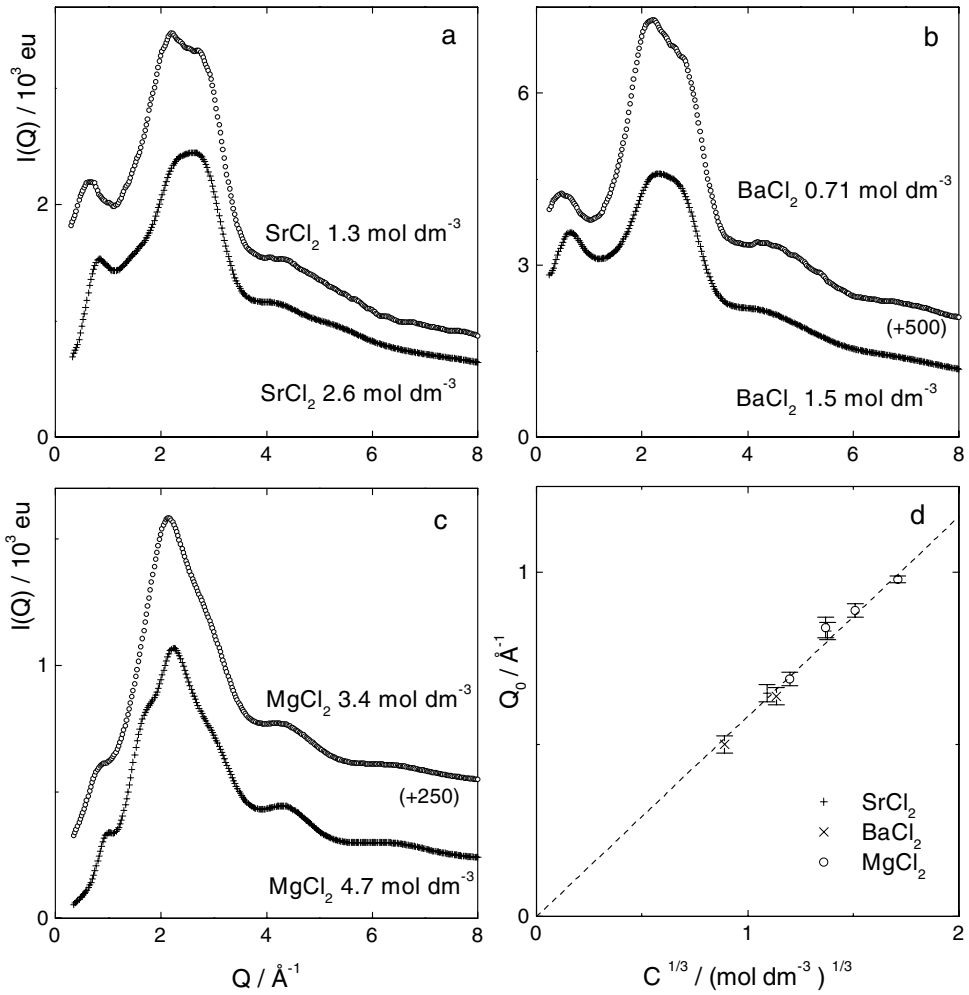


**Figure 5.** X-ray diffraction patterns of strontium, barium, and magnesium chloride aqueous solutions. (a) $SrCl_2$ aqueous solutions: (+) 2.6 mol $dm^{-3}$ and (O) 1.3 mol $dm^{-3}$. (b) $BaCl_2$ aqueous solutions: (+) 1.5 mol $dm^{-3}$ and (O) 0.7 mol $dm^{-3}$. (c) $MgCl_2$ aqueous solutions: (+) 4.7 mol $dm^{-3}$ and (O) 3.4 mol $dm^{-3}$. (d) Variation of the abscissa $Q$ of the first maximum of intensity versus the power 1/3 of the molar concentration. The straight line is calculated considering that the shells of scatterers (hydrated cations) are ordered as a face-centred cubic lattice.

### *3.3. Molecular models: specific comments*

Some specific comments should be given about the solutions investigated. We must initially emphasize that, as a consequence of the solubility of the salts, aqueous solutions of strontium and barium chlorides and bromides close to saturation are still very concentrated (with less than 50 water molecules per cation) but less concentrated than the solutions of trivalent cations (with about ten water molecules per cation). So the number of water molecules outside the first hydration shell is so large that an adequate configuration considered as the result of a plausible local field in these liquid ionic solution cannot be given. For this reason an agreement at low $Q$-values as good as the one obtained for the saturated trivalent cation solutions cannot be expected.

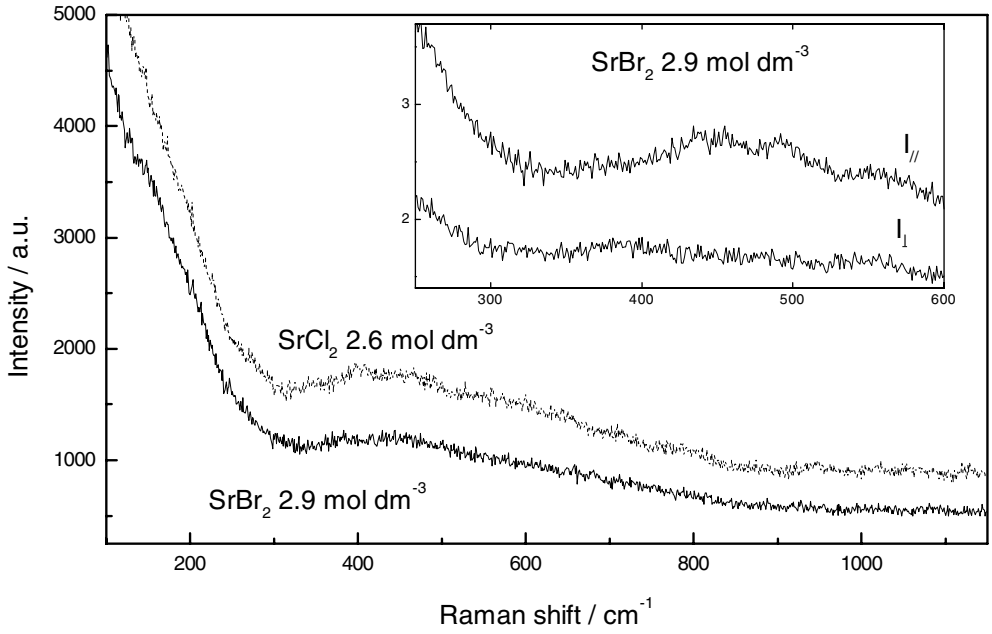


**Figure 6.** Raman spectra of 2.6 mol $dm^{-3}$ $SrCl_2$ and 2.9 mol $dm^{-3}$ $SrBr_2$ aqueous solutions. In the inset the intensities $I_{\parallel}$ and $I_{\perp}$ of the Raman spectra of $SrBr_2$ aqueous solution are shown.

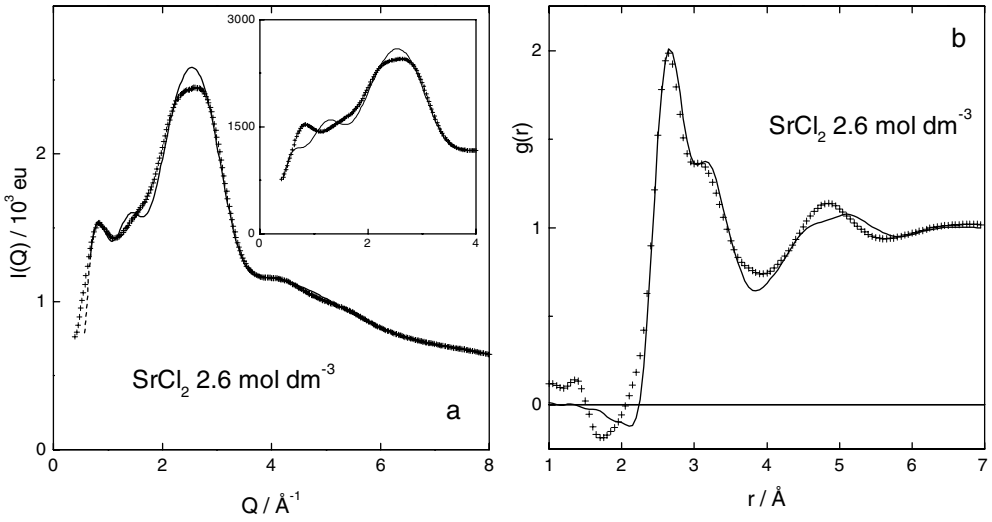


**Figure 7.** The molecular model of the 2.6 mol $dm^{-3}$ $SrCl_2$ aqueous solution. Calculated (——) and experimental (+++): (a) intensities $I_{eu}(Q)$ (the dashed curve shows the calculated intensity for $Q < 1$ $Å^{-1}$); (b) pair correlation function $g(r)$. The inset of (a) shows the intensity calculated from a model were no participation of the closest hydrated cations is considered (see the text).

The molecular models that better reproduce the experimental results are described in the following text. The same kind of hydrate has been used for strontium solutions, taking eight water molecules around the $Sr^{2+}$ cation on a cube position at a distance on average of 2.64 Å for

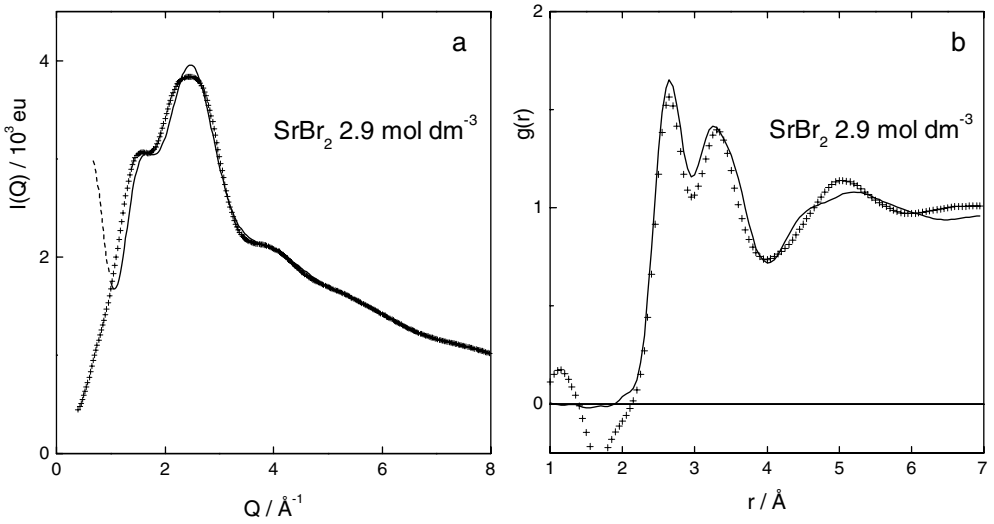


**Figure 8.** The molecular model of the 2.9 mol dm$^{-3}$ $SrBr_2$ aqueous solution. Calculated (——) and experimental (+++): (a) intensities $I_{eu}(Q)$ (the dashed curve shows the calculated intensity for $Q < 1$ Å$^{-1}$); (b) pair correlation function $g(r)$.

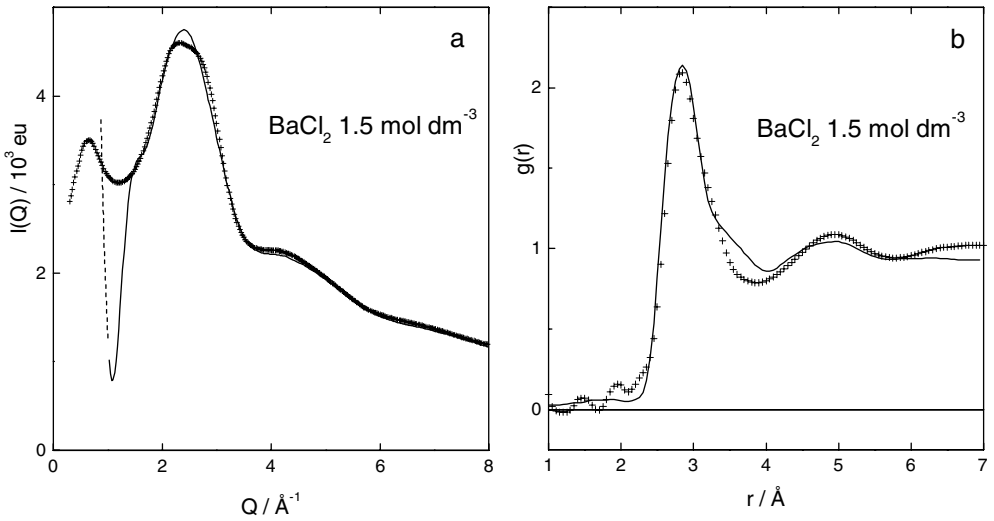


**Figure 9.** The molecular model of the 1.5 mol dm$^{-3}$ $BaCl_2$ aqueous solution. Calculated (——) and experimental (+++): (a) intensities $I_{eu}(Q)$ (the dashed curve shows the calculated intensity for $Q < 1$ Å$^{-1}$); (b) pair correlation function $g(r)$.

both (see table 2(a)). This distance is in agreement with previous x-ray diffraction and EXAFS studies and molecular dynamics simulation for both concentrated [30–35] and very dilute [36] aqueous $SrCl_2$ solutions. Coordination numbers found by various authors of both close to eight [30–33] and ten [34–36] have been reported. The coordination of $Sr^{2+}$ cation obtained by x-ray diffraction and EXAFS on concentrated aqueous solutions of nitrate [37], perchlorate, or trifluoromethane sulphonate [38] appears very similar to that observed on the chloride (eight neighbours at about 2.62 Å). A neutron diffraction study on a concentrated aqueous solution of

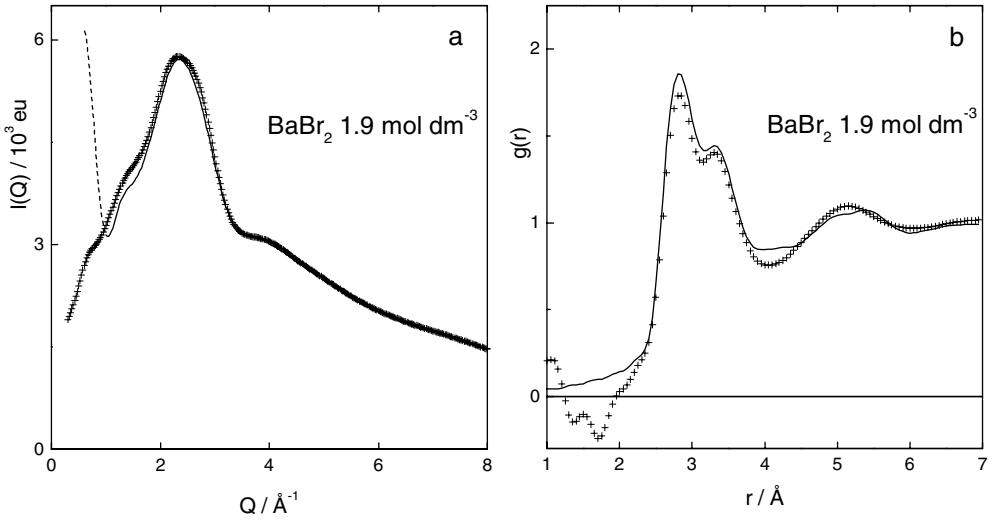


**Figure 10.** The molecular model of the 1.9 mol dm$^{-3}$ $BaBr_2$ aqueous solution. Calculated (——) and experimental (+++): (a) intensities $I_{eu}(Q)$ (the dashed curve shows the calculated intensity for $Q < 1$ Å$^{-1}$); (b) pair correlation function $g(r)$.

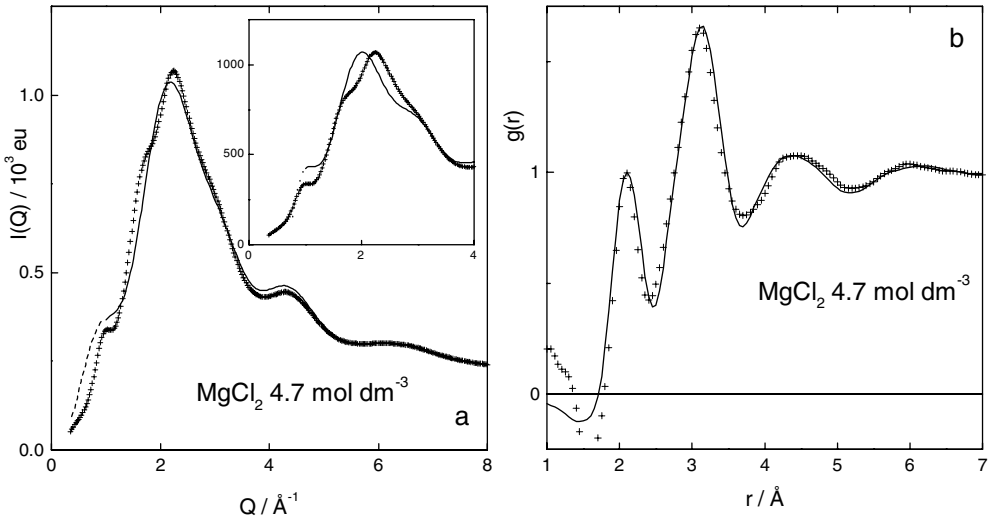


**Figure 11.** Molecular models of the 4.7 mol dm$^{-3}$ $MgCl_2$ aqueous solution. Calculated from model Mg1 (——) and experimental (+++): (a) intensities $I_{eu}(Q)$ (the dashed curve shows the calculated intensity for $Q < 1$ Å$^{-1}$); (b) pair correlation function $g(r)$. The inset of (a) shows the intensity calculated from the model Mg2 (see the text; table 4).

perchlorate, by using the first-order isotope difference method, showed a hydration shell that was not well defined [39]. Our preliminary Raman experiments on $SrCl_2$ and $SrBr_2$ solutions have detected weak and faint bands which cannot plausibly be assigned to a cation hydrate with a well defined structure (figure 6).

Eight water molecules are also located in the first shell of the cation for the barium solutions at an average distance of 2.8 Å. In contrast to the behaviour of the strontium cation,

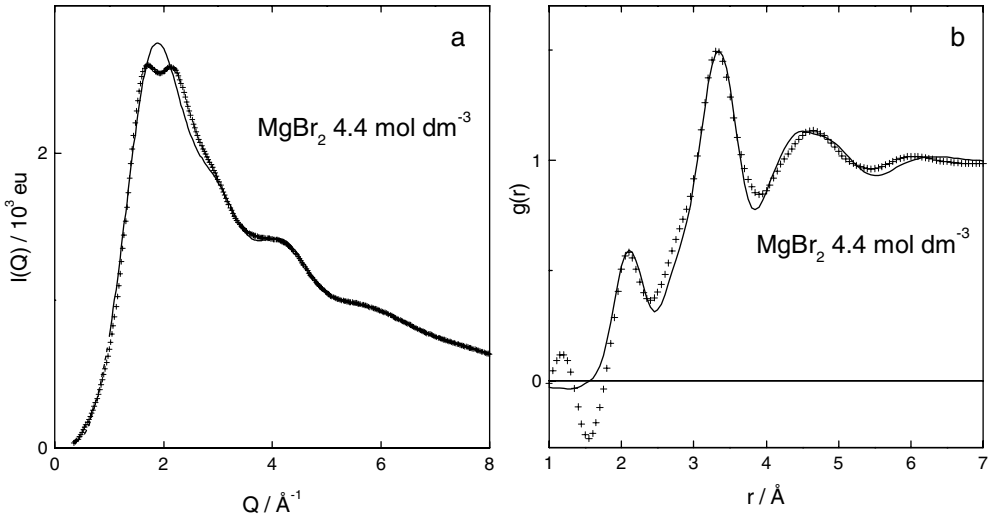


**Figure 12.** The molecular model of the 4.4 mol dm$^{-3}$ $MgBr_2$ aqueous solution. Calculated (——) and experimental (+++): (a) intensities $I_{eu}(Q)$ (the dashed curve shows the calculated intensity for $Q < 1$ Å$^{-1}$); (b) pair correlation function $g(r)$.

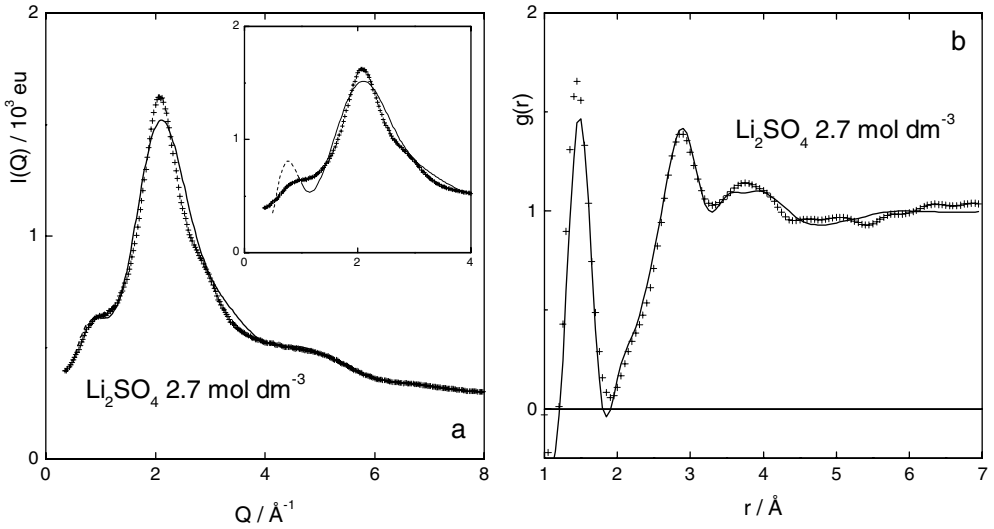


**Figure 13.** Molecular models of the 2.7 mol dm$^{-3}$ $Li_2SO_4$ aqueous solution. Calculated from model Li2 (——) and experimental (+++): (a) intensities $I_{eu}(Q)$ (the dashed curve shows the calculated intensity for $Q < 1$ Å$^{-1}$); (b) pair correlation function $g(r)$. The inset of (a) shows the intensity calculated from the model Li1 (see the text; table 5).

the best fit for the chloride solution was obtained with the water molecules on the vertices of an Archimedean antiprism while for the bromide solution the best agreement is with eight water molecules on the vertices of a cube (see table 3(a)). These results seem to be in agreement with those obtained by Persson *et al* [38] for aqueous $Ba(ClO_4)_2$ solution.

The anions are located between the hydrates: for the strontium chloride solution in the tetrahedral holes of the face-centred cubic structure, while for the strontium bromide and for

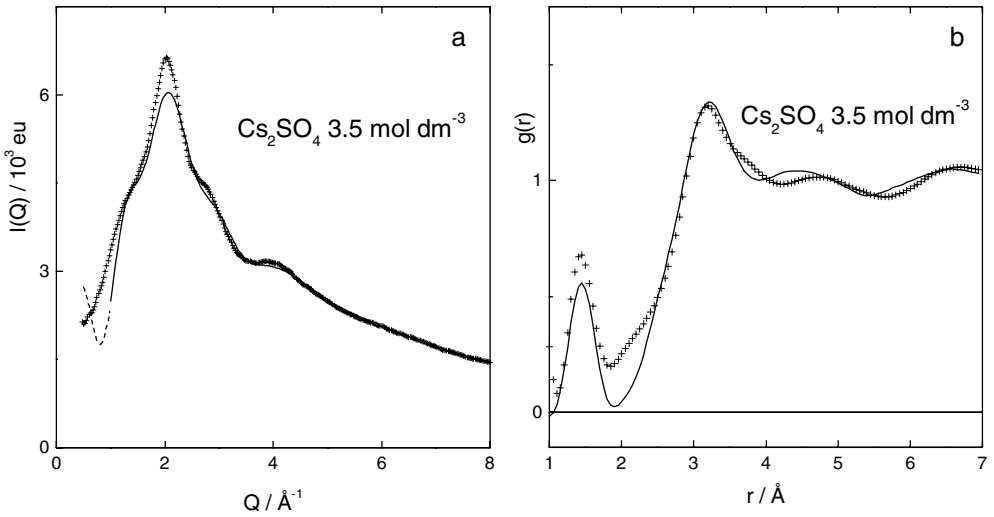


**Figure 14.** Molecular models of the 3.5 mol dm$^{-3}$ $Cs_2SO_4$ aqueous solution. Calculated (——) and experimental (+++): (a) intensities $I_{eu}(Q)$ (the dashed curve shows the calculated intensity for $Q < 1$ Å$^{-1}$); (b) pair correlation function $g(r)$.

the barium halogenide solutions they are located approximately at the mid-points between two cations, although for the bromide aqueous solution these are slightly dislocated in appropriate directions. Where possible, the *free* water molecules have been placed at the middle points between hydrates, and if not they are placed at the remaining vacant sites, on the large octahedral holes of the face-centred cubic structure. Details are given in tables 2(b) and 3(b) and the agreement between the calculated and the experimental intensities and pair correlation functions shown in figures 7 and 10.

The magnesium hydrate used in the molecular models obtained for the most concentrated halide solutions ($10H_2O$ per cation in both solutions) consists of six water molecules at the vertices of a regular octahedron (whose internal positional correlations are presented in table 4(a)) in agreement with results from previous Raman [40] and x-ray diffraction [3, 41–44] experiments. The positional correlations were calculated considering a local close-packing configuration of cation hydrates as described before with the anions slightly dislocated from the middle-point position between the cations. The free water molecules were distributed between the cations and at other vacant sites to fit the available volume. Two models (Mg1 and Mg2) apparently correspond to a plausible description of the arrangements of the ions and water molecules in the aqueous magnesium solution. In model Mg2, the cation–hydration water correlations were considered up to longer distances, which corresponds to a larger overlap of the discrete and continuous distributions. Details are given in table 4(b) where the positional correlations included in the discrete distribution of the molecular models elaborated are indicated together with the value of the threshold of the discrete contribution for each correlation.

For these aqueous solutions a good description of the profile of the experimental intensity was found (figures 11 and 12) also when less than 15% of the closest hydrates were considered in a discrete distribution (see models Mg1 and Mg2). The maximum visible in the profile of the intensity calculated for model Mg2 near to 0.9 Å$^{-1}$ seems to be excessive, while for the pair correlation function no remarkable difference is observed.

To reproduce the experimental intensity for divalent cations and monovalent anions, as discussed before, only a small fraction of the closest hydrates have been considered in a discrete distribution (on average, less than ∼10%). However, the non-existence of discrete

**Table 2.** Structural data for the molecular models for 2.8 mol $dm^{-3}$ $SrCl_2$ and 2.9 mol $dm^{-3}$ $SrBr_2$ aqueous solutions: (a) cation hydrate, (b) the more relevant discrete contributions. Values of the mutual distances $r$, rms fluctuations $\Delta r$, number of particles $w$, and threshold of the continuum $r^{th}$ for each kind of correlation. Distances are in ångströms. (h) means hydration and (f) means *free*.

(a)

| | $Sr^{2+}$ hydrate | | |
|---|---|---|---|
| Correlation | $r$ | $\Delta r$ | $w$ |
| Cation–water (h) | 2.64 | 0.13 | 16 |
| Water (h)–water (h) | 3.05 | 0.16 | 24 |
| | 4.31 | 0.42 | 24 |
| | 5.28 | 0.77 | 8 |

(b)

| | $SrCl_2$ | | | | $SrBr_2$ | | | |
|---|---|---|---|---|---|---|---|---|
| Correlations | $r$ | $\Delta r$ | $w$ | $r^{th}$ | $r$ | $\Delta r$ | $w$ | $r^{th}$ |
| Cation–cation | 9.7 | 1.0 | 0.75 | 6.4 | 9.4 | 1.0 | 0.75 | 6.2 |
| Cation–water (h) | 7.7 | 1.3 | 12 | 6.4 | 7.4 | 1.3 | 12 | 6.2 |
| Water (h)–water (h) | 5.4 | 0.9 | 24 | | 5.0 | 0.6 | 24 | 6.2 |
| | 6.2 | 1.0 | 24 | 6.4 | 5.9 | 0.9 | 24 | |
| Cation–anion | 5.9 | 0.9 | 4 | 5.3 | 4.1 | 0.4 | 4 | 5.2 |
| Cation–water (f) | 4.8 | 0.4 | 24 | | 4.1 | 0.4 | 24 | |
| | 5.8 | 0.9 | 8 | 5.9 | 4.7 | 0.4 | 2 | |
| | | | | | 7.1 | 1.0 | 1 | 5.2 |
| Water (h)–anion | 3.3 | 0.2 | 16 | | 3.4 | 0.3 | 16 | |
| | 5.6 | 0.8 | 16 | 5.3 | 5.4 | 0.4 | 16 | 5.2 |
| Water (h)–water (f) | 3.1 | 0.2 | 48 | | 2.9 | 0.3 | 48 | |
| | 4.0 | 0.5 | 24 | | 3.4 | 0.3 | 8 | |
| | 4.9 | 0.8 | 40 | | 5.4 | 0.5 | 64 | 4.9 |
| | 5.5 | 0.5 | 48 | 5.1 | | | | |
| Anion–water (f) | 3.4 | 0.3 | 24 | | 3.4 | 0.2 | 16 | |
| | 3.7 | 0.3 | 8 | | 3.5 | 0.3 | 4 | |
| | 5.6 | 0.9 | 8 | 5.1 | 5.3 | 0.5 | 8 | 4.8 |
| Anion–anion | 6.8 | 0.9 | | 5.3 | 5.0 | 0.4 | 2 | 5.2 |
| Water (f)–water (f) | 3.3 | 0.3 | 12 | | 3.4 | 0.3 | 8 | |
| | 3.6 | 0.3 | 12 | | 4.7 | 0.4 | 30 | |
| | 4.8 | 0.5 | 30 | | 5.0 | 0.5 | 2 | |
| | 5.3 | 0.8 | 24 | 4.6 | 5.3 | 0.5 | 8 | 4.4 |

correlations between neighbour hydrates leads to a calculated profile which cannot reproduce the experimental intensity. This finding is illustrated for the $SrCl_2$ solution in the inset of figure 7(a).

The decreasing intensity for $Q \sim 1$ Å$^{-1}$ when bromide replaces chloride for the solutions of halogenides of strontium, barium, and magnesium is in agreement with that found previously [3, 19, 21, 45] whenever the anions are not located within the solvation shell of the cation ($AlCl_3$/$AlBr_3$, $MgCl_2$/$MgBr_2$, $YCl_3$/$YBr_3$, $LaCl_3$/$LaBr_3$). This happens because stronger destructive contributions are associated with the anions in that region.

In solutions of lithium sulphate and caesium sulphates the anion is the highest-valence ion and therefore these ions are assumed to be close packed.

The hydration of aqueous solutions of lithium halides has been studied by means of x-ray [46–54] and neutron diffraction [48, 55–61] in addition to computer simulations [52, 53, 62–

**Table 3.** Structural data for the molecular models for 1.5 mol dm$^{-3}$ $BaCl_2$ and 1.9 mol dm$^{-3}$ $BaBr_2$ aqueous solutions: (a) cation hydrates, (b) the more relevant discrete contributions. Values of the mutual distances $r$, rms fluctuations $\Delta r$, number of particles $w$, and threshold of the continuum $r^{th}$ for each kind of correlation. Distances are in ångströms. (h) means hydration and (f) means *free*.

(a)

| | $Ba^{2+}$ hydrate | | | | | |
|---|---|---|---|---|---|---|
| | $BaCl_2$ | | | $BaBr_2$ | | |
| Correlation | $r$ | $\Delta r$ | $w$ | $r$ | $\Delta r$ | $w$ |
| Cation–water (h) | 2.80 | 0.16 | 16 | 2.80 | 0.13 | 16 |
| Water (h)–water (h) | 3.20 | 0.19 | 16 | 3.20 | 0.16 | 24 |
| | 3.70 | 0.26 | 16 | 4.60 | 0.39 | 24 |
| | 4.60 | 0.45 | 8 | 5.60 | 0.52 | 8 |
| | 5.30 | 0.52 | 16 | | | |

(b)

| | $BaCl_2$ | | | | $BaBr_2$ | | | |
|---|---|---|---|---|---|---|---|---|
| Correlations | $r$ | $\Delta r$ | $w$ | $r^{th}$ | $r$ | $\Delta r$ | $w$ | $r^{th}$ |
| Cation–cation | 11.7 | 1.2 | 1 | 8.2 | 10.7 | 1.0 | 1 | 7.4 |
| Cation–water (h) | 9.0 | 0.9 | 4 | | 8.6 | 0.9 | 1 | 6.0 |
| | 9.6 | 1.0 | 12 | 8.2 | | | | |
| Water (h)–water (h) | 6.9 | 0.6 | 16 | | 6.1 | 0.6 | 8 | 6.2 |
| | 7.2 | 0.6 | 4 | | | | | |
| | ... | ... | ... | | | | | |
| | 9.1 | 0.9 | 4 | 8.2 | | | | |
| Cation–anion | 5.9 | 0.6 | 4 | 6.5 | 4.0 | 0.5 | 4 | 5.9 |
| Cation–water (f) | 4.8 | 0.3 | 12 | 3.9 | 5.2 | 0.3 | 24 | 5.2 |
| Water (h)–anion | 3.1 | 0.2 | 2.7 | | 3.3 | 0.2 | 16 | |
| | 3.9 | 0.3 | 8 | | 6.1 | 0.6 | 16 | |
| | 4.8 | 0.6 | 5.3 | | 6.5 | 0.7 | 32 | |
| | ... | ... | ... | | 8.0 | 1.0 | 32 | 8.5 |
| | 6.5 | 0.6 | 16 | 7.9 | | | | |
| Water (h)–water (f) | 3.2 | 0.3 | 32 | 2.7 | 3.5 | 0.2 | 16 | 2.3 |
| Anion–anion | 5.9 | 0.6 | 5.3 | 7.9 | 5.0 | 0.5 | 2.7 | |
| | | | | | 5.7 | 0.6 | 2.7 | |
| | | | | | 7.1 | 0.7 | 0.7 | 8.4 |
| Anion–water (f) | 3.4 | 0.3 | 24 | 3.9 | 3.8 | 0.4 | 16 | 3.6 |
| Water (f)–water (f) | 3.0 | 0.2 | 56 | 3.1 | 3.0 | 0.4 | 32 | 3.2 |

66]. It should be noted that no evidence was detected for the hydration of lithium cations by Raman spectroscopy. Since the scattering power of lithium is very low, only indirect determinations of its hydration are available. The distances and the number of water molecules in the first hydration shell of lithium are strongly dependent on concentration and temperature. Under ambient conditions, e.g. LiCl ($\sim$3 mol dm$^{-3}$), the number of water molecules in the first hydration shell of the cation is about six at a $Li^+$–O distance close to 2.0 Å [55, 61]. A molecular model (Li1) of the $Li_2SO_4$ solution was built assuming that the sulphate anions are correlated at distances calculated as described previously. The lithium hydrates were placed at the mid-points between the anions, while some of the *free* water molecules were very close to the anions and the remaining were in the available positions (water (II) in table 5). In order to reproduce the $g(r)$ function, the lithium hydrate is composed of six water molecules in octahedral positions at

**Table 4.** Structural data for the molecular models for 4.7 mol $dm^{-3}$ $MgCl_2$ and 4.4 mol $dm^{-3}$ $MgBr_2$ aqueous solutions: (a) cation hydrate, (b) the more relevant discrete contributions. Values of the mutual distances $r$, rms fluctuations $\Delta r$, number of particles $w$, and threshold of the continuum $r^{th}$ for each kind of correlation. Distances are in ångströms. (h) means hydration and (f) means *free*.

(a)

| | $Mg^{2+}$ hydrate | | |
|---|---|---|---|
| Correlation | $r$ | $\Delta r$ | $w$ |
| Cation–water (h) | 2.12 | 0.13 | 12 |
| Water (h)–water (h) | 3.00 | 0.16 | 24 |
| | 4.24 | 0.19 | 6 |

(b)

| | $MgCl_2$ | | | | | | | | $MgBr_2$ | | | |
|---|---|---|---|---|---|---|---|---|---|---|---|---|
| | Mg2 | | | | Mg1 | | | | Mg1 | | | |
| Correlations | $r$ | $\Delta r$ | $w$ | $r^{th}$ | $r$ | $\Delta r$ | $w$ | $r^{th}$ | $r$ | $\Delta r$ | $w$ | $r^{th}$ |
| Cation–cation | 7.9 | 0.7 | 6 | 8.4 | 7.9 | 0.8 | 1 | 5.5 | 8.1 | 1.0 | 1 | 5.7 |
| Cation–water (h) | 6.7 | 0.7 | 4 | | 5.9 | 0.4 | 12 | 5.5 | 6.0 | 0.6 | 12 | 5.7 |
| | 8.3 | 0.8 | 4 | | | | | | | | | |
| | 9.2 | 0.9 | 4 | 5.4 | | | | | | | | |
| Water (h)–water (h) | 5.0 | 0.4 | 12 | 4.8 | 3.8 | 0.4 | 3 | | 4.0 | 0.4 | 3 | |
| | | | | | 4.6 | 0.4 | 12 | | 4.8 | 0.4 | 12 | |
| | | | | | 5.0 | 0.4 | 6 | | 5.2 | 0.4 | 6 | |
| | | | | | 5.8 | 0.5 | 6 | | 6.0 | 0.5 | 6 | |
| | | | | | 5.9 | 0.5 | 9 | 5.5 | 6.0 | 0.5 | 9 | 5.7 |
| Cation–anion | 4.3 | 0.4 | 8 | 5.5 | 4.3 | 0.4 | 4 | 4.4 | 4.4 | 0.4 | 4 | 4.5 |
| Cation–water (f) | 4.6 | 0.4 | 24 | 5.4 | 4.2 | 0.4 | 8 | 4.4 | 4.3 | 0.4 | 8 | 4.5 |
| Water (h)–anion | 3.4 | 0.2 | 16 | | 3.1 | 0.2 | 4 | | 3.2 | 0.2 | 4 | |
| | 4.0 | 0.4 | 6 | | 3.3 | 0.2 | 12 | | 3.4 | 0.2 | 12 | |
| | 5.6 | 0.6 | 6 | 5.2 | 4.0 | 0.4 | 4 | | 4.1 | 0.4 | 4 | |
| | | | | | 4.3 | 0.4 | 4 | 4.4 | 4.4 | 0.4 | 4 | 4.5 |
| Water (h)–water (f) | 3.0 | 0.1 | 24 | | 2.7 | 0.1 | 4 | | 2.7 | 0.1 | 4 | |
| | 4.3 | 0.4 | 48 | | 3.2 | 0.2 | 8 | | 3.0 | 0.2 | 8 | |
| | 5.8 | 0.6 | 6 | 5.0 | 3.4 | 0.2 | 12 | | 3.2 | 0.2 | 12 | |
| | | | | | 3.9 | 0.2 | 8 | | 3.8 | 0.2 | 8 | |
| | | | | | 4.1 | 0.4 | 4 | | 4.0 | 0.4 | 4 | |
| | | | | | 4.3 | 0.4 | 4 | | 4.1 | 0.4 | 4 | |
| | | | | | 4.4 | 0.4 | 4 | | 4.3 | 0.4 | 4 | |
| | | | | | 4.7 | 0.4 | 8 | 4.4 | 4.6 | 0.4 | 8 | 4.5 |
| Anion–anion | 3.7 | 0.2 | 0.3 | 3.7 | 4.6 | 0.4 | 4 | 5.0 | 4.7 | 0.4 | 4 | 5.1 |
| Anion–water (f) | 3.9 | 0.3 | 4 | | 3.2 | 0.2 | 2 | | 3.3 | 0.2 | 2 | |
| | 4.7 | 0.4 | 8 | | 3.5 | 0.2 | 4 | | 3.6 | 0.2 | 4 | |
| | 5.1 | 0.6 | 4 | 4.3 | 4.0 | 0.4 | 2 | | 4.1 | 0.4 | 2 | |
| | | | | | 4.5 | 0.4 | 8 | 4.4 | 4.6 | 0.4 | 8 | 4.5 |
| Water (f)–water (f) | 3.2 | 0.2 | 6 | | 2.7 | 0.1 | 3 | | 2.7 | 0.1 | 3 | |
| | 3.4 | 0.4 | 6 | | 3.0 | 0.2 | 2 | | 3.1 | 0.2 | 2 | |
| | 4.7 | 0.4 | 6 | | 3.5 | 0.2 | 4 | | 3.6 | 0.2 | 4 | |
| | 4.8 | 0.5 | 6 | 5.0 | 4.0 | 0.4 | 2 | | 4.1 | 0.4 | 2 | |
| | | | | | 4.5 | 0.4 | 2 | 4.4 | 4.6 | 0.4 | 2 | 4.5 |

**Table 5.** Structural data for the molecular models for 2.7 mol $dm^{-3}$ $Li_2SO_4$ and 3.5 mol $dm^{-3}$ $Cs_2SO_4$ aqueous solutions: the more relevant discrete contributions. Values of the mutual distances $r$, rms fluctuations $\Delta r$, number of particles $w$, and threshold of the continuum $r^{th}$ foe each kind of correlation. Distances are in ångströms. Water (I) for $Li_2SO_4$ solution means hydration water and *free* water for the $Cs_2SO_4$; numbers in parentheses relate to model Li1 discussed in text.

| | $Li_2SO_4$ | | | | $Cs_2SO_4$ | | | |
|---|---|---|---|---|---|---|---|---|
| Correlations | $r$ | $\Delta r$ | $w$ | $r^{th}$ | $r$ | $\Delta r$ | $w$ | $r^{th}$ |
| Anion–anion | | | | | | | | |
| S–S | 9.6 | 1.0 | 0(0.75) | 5.3(6.4) | 8.8 | 0.9 | 1 | 6.1 |
| S–O | 1.5 | 0.1 | 8 | | 1.5 | 0.1 | 8 | |
| | 8.4 | 1.0 | 0(6) | 5.3 (6.4) | 7.6 | 0.8 | 8 | 6.1 |
| O–O | 2.4 | 0.1 | 12 | | 2.4 | 0.1 | 12 | |
| | 7.1 | 1.0 | 0(12) | 5.3 (6.4) | 6.4 | 0.6 | 12 | |
| | | | | | 7.9 | 0.8 | 4 | 6.1 |
| Anion–cation | | | | | | | | |
| S–cation | 4.8 | 0.4 | 4 | 5.3 | 4.2 | 0.4 | 4 | |
| | | | | | 4.5 | 0.4 | 4 | 6.1 |
| O–cation | 4.1 | 0.2 | 16 | 5.3 | 3.2 | 0.3 | 4 | |
| | | | | | 3.4 | 0.3 | 4 | |
| | | | | | ... | ... | ... | |
| | | | | | 5.5 | 0.6 | 4 | 5.8 |
| Anion–water (I) | | | | | | | | |
| S–water (I) | 3.6 | 0.3 | 16 | | 4.3 | 0.4 | 12 | |
| | 5.2 | 0.6 | 8 | 5.3 | 5.4 | 0.6 | 16 | |
| | | | | | 6.5 | 0.6 | 48 | 8.1 |
| O–water (I) | 2.8 | 0.1 | 16 | | 3.7 | 0.3 | 24 | |
| | 3.5 | 0.2 | 16 | | 3.9 | 0.3 | 8 | |
| | 4.2 | 0.2 | 16 | | 5.1 | 0.5 | 24 | |
| | ... | ... | ... | | 5.3 | 0.5 | 24 | |
| | 5.0 | 0.6 | 16 | 5.3 | ... | ... | ... | |
| | | | | | 7.2 | 0.7 | 48 | 7.7 |
| Anion–water (II) | | | | | | | | |
| S–water (II) | 3.4 | 0.2 | 2 | | 4.4 | 0.4 | 16 | |
| | 4.0 | 0.2 | 4 | | 7.6 | 0.8 | 32 | 8.8 |
| | 4.8 | 0.3 | 4 | | | | | |
| | 6.1 | 0.6 | 8 | 5.7 | | | | |
| O–water (II) | 2.8 | 0.1 | 4 | | 3.3 | 0.1 | 16 | |
| | 3.7 | 0.2 | 16 | | 4.6 | 0.4 | 32 | |
| | 4.0 | 0.2 | 4 | | 5.6 | 0.6 | 16 | |
| | 4.4 | 0.3 | 4 | | ... | ... | ... | |
| | ... | ... | ... | | 7.0 | 0.7 | 32 | 7.4 |
| | 6.8 | 0.8 | 8 | 5.7 | | | | |
| Cation–water (I) | 2.1 | 0.1 | 24 | 4.2 | 3.1 | 0.3 | 8 | |
| | | | | | 3.3 | 0.3 | 8 | |
| | | | | | 3.4 | 0.3 | 8 | |
| | | | | | 4.8 | 0.5 | 16 | 5.2 |
| Cation–water (II) | 3.7 | 0.2 | 4 | | 4.3 | 0.4 | 11 | |
| | 4.4 | 0.3 | 2 | | 4.5 | 0.4 | 11 | |
| | 4.8 | 0.3 | 2 | | 6.1 | 0.6 | 5 | 6.4 |
| | 5.0 | 0.6 | 2 | 3.7 | | | | |
| Water (I)–water (I) | 2.9 | 0.1 | 48 | | 2.8 | 0.1 | 24 | |

**Table 5.** (Continued.)

| | $Li_2SO_4$ | | | | $Cs_2SO_4$ | | | |
|---|---|---|---|---|---|---|---|---|
| Correlations | $r$ | $\Delta r$ | $w$ | $r^{th}$ | $r$ | $\Delta r$ | $w$ | $r^{th}$ |
| | 4.2 | 0.2 | 12 | 4.2 | 3.8 | 0.3 | 6 | |
| | | | | | 4.6 | 0.4 | 48 | |
| | | | | | 6.2 | 0.6 | 12 | |
| | | | | | 6.6 | 0.7 | 48 | 6.4 |
| Water (I)–water (II) | 2.8 | 0.1 | 8 | | 3.1 | 0.1 | 16 | |
| | 3.2 | 0.2 | 4 | | 3.3 | 0.4 | 32 | |
| | 3.4 | 0.2 | 8 | | 4.8 | 0.5 | 32 | |
| | ... | ... | ... | | 5.9 | 0.6 | 32 | |
| | 4.9 | 0.6 | 4 | 3.8 | 6.1 | 0.6 | 32 | 5.0 |
| Water (II)–water (II) | 2.8 | 0.1 | 4 | | 4.4 | 0.4 | 21 | |
| | 2.9 | 0.1 | 1 | | 6.2 | 0.6 | 16 | 6.6 |
| | 3.4 | 0.2 | 2 | | | | | |
| | ... | ... | ... | | | | | |
| | 7.3 | 0.9 | 1 | 4.3 | | | | |

a distance on average of 2.10 Å (water (I) in table 5). A good agreement is obtained for $g(r)$ and for the experimental intensity (figure 13). However, the *pre-peak* appears overestimated even with a small fraction (6%) of the closest hydrates considered in a discrete distribution. Better agreement is obtained with the experimental intensity close to 1 $Å^{-1}$ using a similar molecular model but without correlations between the sulphate anions, model Li2 (figure 13(a)). This, however, does not allow us to draw conclusions on the relevance of the positional correlations between the anions.

For aqueous solutions of caesium sulphate (figure 14), the caesium cation is assumed (in the model) to be at the mid-point between two sulphate anions slightly displaced towards the anion.

The number of water molecules in the first shell of caesium is 8, with reported distances varying between 3.1 and 3.4 Å (water I in table 5). These values are consistent with those found for caesium halides obtained by x-ray [47, 67], neutron diffraction [68], and molecular dynamics studies [62, 69]. The maximum of the interferences corresponding to positional correlations at distances of about 8.8 Å is not visible in the profile of the experimental intensity near $Q \sim 0.9$ $Å^{-1}$, because destructive interference originated by the correlations $Cs^+$–$SO_4^{2-}$ occurs. This interpretation is in agreement with what is observed when the x-ray diffraction patterns of solutions of bromides are compared with the corresponding patterns of chlorides (the referred reduction of the intensity of the maxima observed near 1 $Å^{-1}$).

The solvation shell of the sulphate anion is clearly not as tight as those observed with the trivalent cations previously reported by us [13, 17, 19–21]. The value of the electrostatic field in the vicinity of the anion is weaker both because the sulphate anion is divalent and because it is very large. The competition between the ions in coordinating water molecules is, therefore, not as efficient in producing the (quasi-) close packing as was reasonably suggested for the trivalent cations. Very good agreement cannot therefore be obtained between the profile of the experimental intensity and that calculated from our models assuming as strict a (quasi-) close-packing structure as was used for trivalent cations. However, the agreement was tested for $Q$-values near 0.9 $Å^{-1}$ corresponding to positional correlations at distances approaching the (sulphate) anion–(sulphate) anion minimum value assuming these anions to be close packed. Less than 10% of the sulphate anions were included in the discrete distributions.

## 4. Conclusions

A quasi-close-packed structure of divalent ions has been shown to interpret satisfactorily the profile of the x-ray intensity observed for a large range of $Q$-values (from $\sim$1 Å$^{-1}$ up to high values) for the concentrated aqueous solutions studied, of salts consisting by divalent ions combined with monovalent counter-ions. However, only a few (generally less than 10%) of the molecules or ions integrated within the solvated divalent ions seem to be representative of this quasi-close-packed structure. This demonstrates a drastic reduction of the participation of the molecules and ions belonging to the hydrates compared with what was proposed using molecular models built by us to simulate the structure of solutions of salts consisting of trivalent (ions) combined with monovalent ions [13, 17, 19–21]. For these solutions, between 35 and 50% of the constituents of the trivalent ion complexes are included in discrete distributions while the remaining hydration shells merge into a continuum. The reduced participation in discrete distributions that produce the interferences observed at low $Q$-values in the x-ray patterns seems to be in agreement with the reduction (from *three* to *two*) of the value of the intensity of the electrostatic field created by the ions of high valence that constitute the dissolved salt. The relevance of the value of the electric charge of one of the ions in the organization of a *quasi-close-packing* structure can also be emphasized by comparing the results obtained for the electrolytes studied here with the results for other solutions. In the x-ray diffraction patterns of concentrated aqueous solutions of salts containing exclusively monovalent ions, a *pre-peak* is never observed. So the existence of any *quasi-close-packing* structure of cations or anions does not seem to be plausible in these ionic liquids.

In short, the maxima of interference at low $Q$-values (the *first sharp diffraction peaks* referred to in research on the structure of melts and glasses [70–80]) result from the cooperation of x-rays scattered from slight accumulations of molecules and ions in clouds that are centred in the quasi-close-packed positions of the ions of high valence. This subtle accumulation of scattering power certainly cannot be adequately described by our models using only discrete distributions. In general terms, we may state that the existence of a contrast in values of scattering power between spatial domains of the solution that are approximately close packed and those ascribed to the *holes* of this quasi-close packing is the ultimate interpretation of the existence of the *first sharp diffraction peak* for these concentrated aqueous solutions.

## Acknowledgments

The authors are pleased to thank Dr Thomas Buslaps and Dr Veijo Honkimaki for their assistance with beamline ID15b during the x-ray diffraction experiments at ESRF, as well as Professor Rui de Almeida for Raman facilities and Ms Isabel Nogueira for her assistance during these experiments. The authors thank Dr Maria Luisa Almeida who calculated some models, and Ms Maria Clara Carreiro da Costa, who prepared and analysed the solutions investigated, is also acknowledged. Professor H D Burrows of Universidade de Coimbra is thanked for reading the manuscript.

We thank 'Fundação Calouste Gulbenkian' and 'Electricidade de Portugal (EDP)' for having financed the acquisition of some equipment (a powerful $Ar^+$ laser) for the experiments. A M Gaspar acknowledges the financial support given by 'Fundação para a Ciência e Tecnologia'.

## References

[1] Prins J A and Fonteyne R 1935 *Physica* **2** 1016
Prins J A and Fonteyne R 1935 *J. Chem. Phys.* **3** 72 and references therein
[2] Dorosh A K and Skryshevskii A F 1967 *Zh. Strukt. Khim.* **8** 3408

[3] Alves Marques M and de Barros Marques M I 1974 *Proc. K. Ned. Akad. Wet.* B **77** 286
[4] Howe R A, Howells W S and Enderby J E 1974 *J. Phys. C: Solid State Phys.* **7** L111
[5] Enderby J E 1975 *Proc. R. Soc.* A **345** 107
[6] Neilson G W, Howe R A and Enderby J E 1975 *Chem. Phys. Lett.* **33** 284
[7] Caminiti R, Licheri G, Piccaluga G and Pinna G 1979 *Rev. Inorg. Chem.* **333**
[8] Licheri G, Piccaluga G and Pinna G 1979 *J. Am. Chem. Soc.* **101** 5438
[9] Enderby J E and Neilson G W 1980 *Adv. Phys.* **29** 323
[10] Habenschuss A and Spedding F H 1980 *J. Chem. Phys.* **73** 442
[11] Soper A K, Enderby J E and Neilson G W 1981 *Rep. Prog. Phys.* **44** 595
[12] Pálinkás G and Kalman E 1981 *Z. Naturf.* a **36** 1367
[13] de Barros Marques M I, Cabaço M I, de Sousa Oliveira M A and Alves Marques M 1982 *Chem. Phys. Lett.* **91** 222
[14] Magini M, Paschina G and Piccaluga G 1982 *J. Chem. Phys.* **76** 1116 and references therein
[15] Neilson G W and Enderby J E 1983 *Proc. R. Soc.* A **390** 353
[16] Iijima T and Nishikawa K 1985 *Chem. Phys. Lett.* **115** 522
[17] Alves Marques M and Cabaço M I 1986 *Chem. Phys. Lett.* **123** 73
Alves Marques M and Cabaço M I 1986 *Chem. Phys. Lett.* **124** 487
[18] Meier W, Bopp P, Probst M M, Spohr E and Lin J-L 1990 *J. Phys. Chem.* **94** 4672
[19] Cabaço M I, Alves Marques M, de Barros Marques M I, Bushnell-Wye G, Costa M M R, de Almeida M J and Andrade L C 1995 *J. Phys.: Condens. Matter* **7** 7409
[20] Cabaço M I, Gaspar A M, de Morais C M and Alves Marques M 2000 *J. Phys.: Condens. Matter* **12** 2623
[21] Alves Marques, Cabaço M I, de Barros Marques M I, Gaspar A M and de Morais C M 2001 *J. Phys.: Condens. Matter* **13** 4367
[22] Mills R, March N H, Giaquinta P V, Parrinello M and Tosi M P 1977 *Chem. Phys.* **26** 237
[23] Krogh–Moe J 1956 *Acta Crystallogr.* **9** 951
Norman N 1957 *Acta Crystallogr.* **10** 370
[24] Warren B E 1968 *X-ray Diffraction* (Reading, MA: Addison-Wesley)
[25] Wilson A J C (ed) 1992 *International Tables for Crystallography* C
[26] Pálinkás G 1973 *Acta Crystallogr.* A **29** 10
[27] Pálinkás G and Radnai T 1976 *Acta Crystallogr.* A **32** 666
[28] Hajdu F 1972 *Acta Crystallogr.* A **28** 250
[29] Narten A H, Danford M D and Levy H A 1967 *Discuss. Faraday Soc.* **43** 97
[30] Albright J N 1972 *J. Chem. Phys.* **56** 3783
[31] Caminiti R, Musini A, Paschina G and Pinna G 1982 *J. Appl. Crystallogr.* **15** 482
[32] Parkman R H, Charnock J M, Livens F R and Vaughan D J 1998 *Geochim. Cosmochim. Acta* **62** 1481
[33] Seward T M, Henderson C M B, Charnock J M and Driesner T 1999 *Geochim. Cosmochim. Acta* **63** 2409
[34] Spohr E, Pálinkás G, Heinzinger K, Bopp P and Probst M M 1988 *J. Phys. Chem.* **92** 6754
[35] D'Angelo P, Nolting H-F and Pavel N V 1996 *Phys. Rev.* A **53** 798
[36] O'Day P A, Newville M, Neuhoff P S, Sahai N and Carroll S A 2000 *J. Colloid Interface Sci.* **222** 184
[37] Pfund D M, Darab J G, Fulton J L and Ma Y 1994 *J. Phys. Chem.* **98** 13 102
[38] Persson I, Sandström M, Yokohama H and Chaudhry M 1995 *Z. Naturf.* a **50** 21
[39] Neilson G W and Broadbent R D 1990 *Chem. Phys. Lett.* **167** 429
[40] da Silveira A, Alves Marques M and Macias Marques N 1965 *Mol. Phys.* **9** 271
[41] Dorosh A K and Skryshevskii A F 1964 *J. Struct. Chem.* **5** 842
[42] Caminiti R, Licheri G, Piccaluga G and Pinna G 1979 *J. Appl. Crystallogr.* **12** 34
Caminiti R, Licheri G, Piccaluga G and Pinna G 1979 *Chem. Phys. Lett.* **61** 45
[43] Caminiti R, Licheri G, Paschina G, Piccaluga G and Pinna G 1980 *Z. Naturf.* a **35** 1361
[44] Pálinkás G, Radnai T, Dietz W, Szász G I and Heinzinger K 1982 *Z. Naturf.* a **37** 1049
[45] de Barros Marques M I 1983 *Thesis* Universidade de Lisboa
[46] Brady G W 1958 *J. Chem. Phys.* **28** 464
[47] Lawrence R M and Kruh R F 1967 *J. Chem. Phys.* **47** 4758
[48] Narten A H, Vaslow F and Levy H A 1973 *J. Chem. Phys.* **58** 5017
[49] Licheri G, Piccaluga G and Pinna G 1975 *Chem. Phys. Lett.* **35** 119
[50] Caminiti R, Licheri G, Piccaluga G and Pinna G 1975 *Ann. Chim.* **65** 695
[51] Pálinkás G, Radnai T and Hajdu F 1980 *Z. Naturf.* a **35** 107
[52] Radnai T, Pálinkás G, Szász G I and Heinzinger K 1981 *Z. Naturf.* a **36** 1076
[53] Tanaka K, Ogita N, Tamura Y, Okada I, Ohtaki H, Pálinkás G, Spohr E and Heinzinger K 1987 *Z. Naturf.* a **42** 29

[54] Tamura Y, Yamaguchi T, Okada I and Ohtaki H 1987 *Z. Naturf.* a **42** 367
[55] Newsome J R, Neilson G W and Enderby J E 1980 *J. Phys. C: Solid State Phys.* **13** L923
[56] Ichikawa K, Kameda Y, Matsumoto T and Misawa M 1984 *J. Phys. C: Solid State Phys.* **17** L725
[57] Copestoke A P, Neilson G W and Enderby J E 1985 *J. Phys. C: Solid State Phys.* **18** 4211
[58] Cartailler T, Kunz W, Turq P and Bellissent-Funel M-C 1991 *J. Phys.: Condens. Matter* **3** 9511
[59] Yamagami M, Yamaguchi T, Wakita H and Misawa M 1994 *J. Chem. Phys.* **100** 3122
[60] Yamaguchi T, Yamagami M, Wakita H and Soper A 1995 *J. Mol. Liq.* **65/66** 91
[61] Howell I and Neilson G W 1996 *J. Phys.: Condens. Matter* **8** 4455
[62] Heinzinger K and Vogel P C 1974 *Z. Naturf.* a **29** 1164
Heinzinger K and Vogel P C 1976 *Z. Naturf.* a **31** 463
[63] Clementi E and Barsotti R 1978 *Chem. Phys. Lett.* **59** 21
[64] Szász G I, Heinzinger K and Pálinkás G 1981 *Chem. Phys. Lett.* **78** 194
[65] Bopp P, Okada I, Ohtaki H and Heinzinger K 1985 *Z. Naturf.* a **40** 116
[66] Heinzinger K 1985 *Pure Appl. Chem.* **57** 1031
[67] Bertagnolli H, Weidner J U and Zimmerman H W 1974 *J. Chem. Phys.* **47** 4758
Bertagnolli H, Weidner J U and Zimmerman H W 1974 *Ber. Bunsenges. Phys. Chem.* **78** 2
[68] Ohtomo N and Arakama K 1979 *Bul. Chem. Soc. Japan* **52** 2755
[69] Briant C L and Burton J J 1976 *J. Chem. Phys.* **64** 2888
[70] Price D L, Moss S C, Reijers R, Saboungi M L and Susman S 1989 *J. Phys.: Condens. Matter* **1** 1005
[71] Penfold I T and Salmon P S 1991 *Phys. Rev. Lett.* **67** 97
[72] Salmon P S 1992 *Proc. R. Soc.* A **437** 591
[73] Elliot S R 1992 *J. Phys.: Condens. Matter* **4** 7661 and references therein
[74] Tosi M P, Price D L and Saboungi M L 1993 *Ann. Rev. Phys. Chem.* **44** 173
[75] Salmon P S 1994 *Proc. R. Soc.* A **445** 351
[76] Wasse J C and Salmon P S 1998 *J. Phys.: Condens. Matter* **11** 1389
[77] Wasse J C and Salmon P S 1999 *J. Phys.: Condens. Matter* **11** 9293
[78] Tosi M P 1999 *J. Mol. Liq.* **83** 23 and references therein
[79] Lin Z, Youshi W, Xiufang B, Hui L, Weimin W, Jingguo L and Ning L 1999 *J. Phys.: Condens. Matter* **11** 7959 and references therein
[80] Wilson M and Madden P A 1998 *Phys. Rev. Lett.* **80** 532